Monte Carlo studies of the spontaneous rotational symmetry breaking in dimensionally reduced super Yang-Mills models

Konstantinos N. Anagnostopoulos,[a] **Takehiro Azuma**[b] **and Jun Nishimura**[c,d]

[a] *Physics Department, National Technical University,*
Zografou Campus, GR-15780 Athens, Greece

[b] *Institute for Fundamental Sciences, Setsunan University,*
17-8 Ikeda Nakamachi, Neyagawa, Osaka, 572-8508, Japan

[c] *KEK Theory Center, High Energy Accelerator Research Organization,*
1-1 Oho, Tsukuba, Ibaraki, 305-0801, Japan

[d] *Department of Particle and Nuclear Physics,*
Graduate University for Advanced Studies (SOKENDAI),
1-1 Oho, Tsukuba, Ibaraki, 305-0801, Japan

E-mail: konstant@mail.ntua.gr, azuma@mpg.setsunan.ac.jp, jnishi@post.kek.jp

ABSTRACT: It has long been speculated that the spontaneous symmetry breaking (SSB) of $SO(D)$ occurs in matrix models obtained by dimensionally reducing super Yang-Mills theory in $D = 6, 10$ dimensions. In particular, the $D = 10$ case corresponds to the IIB matrix model, which was proposed as a nonperturbative formulation of superstring theory, and the SSB may correspond to the dynamical generation of four-dimensional space-time. Recently, it has been shown by using the Gaussian expansion method that the SSB indeed occurs for $D = 6$ and $D = 10$, and interesting nature of the SSB common to both cases has been suggested. Here we study the same issue from first principles by a Monte Carlo method in the $D = 6$ case. In spite of a severe complex-action problem, the factorization method enables us to obtain various quantities associated with the SSB, which turn out to be consistent with the previous results obtained by the Gaussian expansion method. This also demonstrates the usefulness of the factorization method as a general approach to systems with the complex-action problem or the sign problem.

Contents

1 Introduction

Monte Carlo calculations in lattice gauge theories have played an important role in nonperturbative studies of QCD. Similar progress has started to take place in the study of nonperturbative effects in superstring theory using matrix models. (See ref. [1] for a comprehensive review.) Such effects are thought to play a crucial role in the choice of the true vacuum in the string landscape. The most fundamental problem is the determination of the macroscopic space-time dimensionality, which should turn out to be lower than the space-time dimensionality of the full theory.

The IIB matrix model [2] has been conjectured to define superstring theory nonperturbatively in a properly taken large-N limit of the $N \times N$ matrices. Using dualities, it is expected that the model describes the unique underlying theory in spite of its explicit connection to perturbative type IIB superstring theory. The model is defined originally in 10 dimensions and it has only one scale, even after taking quantum effects into consideration, which raises the possibility that there is a unique true vacuum. Space-time in this model arises dynamically from the eigenvalue distribution of the ten bosonic matrices A_μ [3]. It is therefore possible to realize dynamical compactification of the extra dimensions and to obtain a macroscopic four-dimensional space-time.[1]

Originally the IIB matrix model has been studied in its Euclidean version mainly because quantum effects render the partition function of the model finite despite the flat

---

[1] A closely related idea in superstring theory is to realize an "emergent space-time" in the context of gauge-gravity duality [4, 5]. To test this idea, Monte Carlo studies [6–14] have been performed on the one-dimensional reduction of the ten-dimensional $\mathcal{N} = 1$ U(N) super Yang-Mills theory, which provides a low energy description of a stack of N D0 branes in type IIA superstring theory. In particular, the black hole thermodynamics has been reproduced from Monte Carlo studies of the gauge theory [10] *including α' corrections*, which correspond to the effects of closed strings with finite length. Wilson loops and correlation functions of the strongly coupled gauge theory can be calculated more simply on the gravity side [15, 16], and these predictions have been confirmed by Monte Carlo simulations on the gauge theory side [12–14].

directions in the action [17, 18]. Using the Gaussian expansion method (GEM) [19, 20], it was shown that dynamical compactification is realized by spontaneously breaking the SO(10) rotational symmetry of the model, giving rise to an SO(3) symmetric vacuum [21]. Moreover, SO(d) symmetric vacua in general were found to have a universal scale r for the small dimensions and a scale R_d for the large dimensions satisfying $(R_d)^d r^{10-d} = \ell^{10}$ with some dynamical scale ℓ, resulting in constant volume and a finite ratio R_d/r. The scenario of dynamical compactification via SSB was conjectured earlier based on the low-energy effective theory [3] and the effects of the fermionic partition function [22, 23].

A more exciting scenario has been discovered recently by a Monte Carlo study of the *Lorentzian* version of the IIB matrix model [24]. The model was not studied before beyond the classical level [25, 26] because it seemed unstable due to the non-positive-definite bosonic action $S_{\rm b}$ and the phase factor $e^{iS_{\rm b}}$. Using simple scaling properties of the model, it was possible to integrate out $e^{iS_{\rm b}}$ yielding a constraint $S_{\rm b} \approx 0$. Contrary to the Euclidean model, one needs to introduce large scale cutoffs in the temporal and spatial extents $\frac{1}{N}\text{tr}(A_0)^2$ and $\frac{1}{N}\text{tr}(A_i)^2$, which can be removed in the large-N limit. Remarkably, it was found that a (3+1)-dimensional *expanding* universe emerges dynamically after a critical time. Before this time, space is SO(9) symmetric and small. After this time, 3 dimensions of space expand rapidly signaling the birth of the universe. Emergence of time happens nontrivially due to a crucial role played by supersymmetry, whereas non-commutativity of space plays an important role in the SSB of SO(9) rotational symmetry leading to an SO(3) symmetric space of large dimensions. Refs. [27, 28] investigated classical equations of motion, which are expected to be valid at late times, and presented interesting solutions which represent a (3+1)-dimensional expanding universe with zero space-time non-commutativity. This result points to the possibility that space-time non-commutativity disappears at some point in time. Ref. [29] has proposed a procedure to identify the local fields corresponding to the massless modes that appear at late times. The possibility that the Standard Model emerges at low energy from the IIB matrix model has been discussed in refs. [30–32].

Monte Carlo studies of the Euclidean IIB and related matrix models, on the other hand, have been pursued for more than fifteen years. Small matrices were originally studied in ref. [17] and the large-N limit of matrix models without fermions was studied in ref. [33]. The large-N limit of a four-dimensional version of the IIB matrix model was first studied in ref. [34]. Simulations of the IIB matrix model and its six-dimensional version suffer from a strong complex-action problem. After integrating out the fermionic matrices, the complex fermionic partition function is found to have a wildly fluctuating phase.[2] A phase-quenched model with oneloop approximation was studied by Monte Carlo simulation in ref. [35]. In such models *without* complex action, however, it is strongly suggested that SSB does not occur [33–36]. Therefore, the complex phase is expected to play a central role if the SSB really occurs in the Euclidean IIB matrix model. These early studies, as well as simulations performed in refs. [37, 38], provided a lot of insights into the large-N

---

[2]The fermionic partition function is real in the Lorentzian IIB matrix model, which can therefore be studied by Monte Carlo simulation without the complex-action problem [24].

limit and the nonperturbative dynamics of the Euclidean IIB matrix model.

In order to overcome the complex-action problem, ref. [23] proposed the so-called factorization method, which has the advantage of being quite general. It was tested on simple models [39–43] and used in simulations of finite density QCD [44] (see refs. [45, 46] for related works on the QCD phase diagram and refs. [47] for other approaches to the complex-action problem). While the actual calculations resemble the density of states methods [48] proposed earlier, the crucial point of the new approach is to constrain *all* the independent observables that are strongly correlated with the phase fluctuations as was first recognized in refs. [42, 43]. By numerically determining the minimum of the free energy with respect to these observables, it is possible to sample efficiently the configurations which give the most important contributions to the partition function.

For the IIB matrix model, the choice of observables can be made in a rather intuitive way. In ref. [22] it is shown that the complex phase vanishes for dimensionally collapsed configurations and that the phase is stationary with respect to fluctuations around them. It is therefore possible that such configurations are favored despite their entropic suppression. In a simplified matrix model for dynamical compactification proposed in ref. [49], we have found strong evidence [42, 43] that the length scales in each dimension are the *only* relevant observables that have an important correlation with the complex phase. Monte Carlo calculations of the simplified model indeed reproduced various quantities associated with the SSB obtained earlier by the GEM [50].

In this paper we perform Monte Carlo studies of the six-dimensional version of the Euclidean IIB matrix model. The model is supersymmetric, and the space-time emerges dynamically from the eigenvalue distribution of the bosonic matrices. Using the GEM, ref. [51] showed that dynamical compactification of the extra dimensions occurs via SSB of SO(6) rotational symmetry to an SO(3) symmetric vacuum. Similarly to the ten-dimensional model [21], SO(d) symmetric vacua in general were found to have a universal scale r for the small dimensions and a scale R_d for the large dimensions satisfying $(R_d)^d r^{6-d} = \ell^6$ with some dynamical scale ℓ, resulting in constant volume and a finite ratio R_d/r. In ref. [23], simulations of this model using the oneloop approximation revealed the strong effect of the fluctuations of the phase in generating the scales r and R_d. We will show, however, that this approximation fails to capture the short distance nonperturbative dynamics of the eigenvalues of the matrices, which play a crucial role in actual determination of the scales r and R_d. In fact we find a strong, nonperturbative, hard core potential against the collapse of the eigenvalues that leads to nontrivial solutions for r in the large-N limit. Simulating the full model, however, requires $\mathcal{O}(N^2)$ additional computational effort, and state-of-the-art algorithms used in lattice QCD simulations with dynamical fermions have to be used in order to make calculations feasible. We are able to compute expectation values based on the factorization method using scaling properties of the distribution functions in order to extrapolate efficiently to the region of configuration space favored at large N. These scaling properties are similar to the ones found in the simplified model [42, 43]. Our final results are consistent with the GEM predictions for the universal scale r and the constant volume property. Some preliminary results of this work have been presented in a proceeding contribution [52].

This paper is organized as follows. In section 2 we describe the model and review the previous results obtained by the GEM. In section 3 we explain the complex-action problem and discuss how it can be overcome by using the factorization method. In section 4 we describe our simulations and present our numerical results. Section 5 is devoted to a summary and discussions. The details of the algorithm used in the Monte Carlo simulation are given in appendix A.

2 The model and a brief review of previous results

The IIB matrix model is formally obtained by the dimensional reduction of $D = 10$, $\mathcal{N} = 1$, $\mathrm{SU}(N)$ super Yang-Mills theory [2]. After the reduction, the $\mathcal{N} = 1$ supersymmetry is enhanced to $\mathcal{N} = 2$ supersymmetry, which leads to the interpretation of the eigenvalues of A_μ as the ten-dimensional space-time coordinates [2, 3]. Therefore, space-time is generated *dynamically* although it is generically non-commutative since dominant configurations in the large-N limit may consist of non-simultaneously-diagonalizable matrices [34].

In this paper we study a $D = 6$ version of the IIB matrix model, whose partition function is given by

$$Z = \int dA \, d\psi \, d\bar{\psi} \, \mathrm{e}^{-S_\mathrm{b} - S_\mathrm{f}} \ ,$$

$$S_\mathrm{b} = -\frac{1}{4g^2} \mathrm{tr} \, [A_\mu, A_\nu]^2 \ ,$$

$$S_\mathrm{f} = -\frac{1}{2g^2} \mathrm{tr} \, \left(\bar{\psi}_\alpha (\Gamma_\mu)_{\alpha\beta} [A_\mu, \psi_\beta] \right) \ . \tag{2.1}$$

The $N \times N$ matrices A_μ ($\mu = 1, \ldots, 6$) are traceless and Hermitian, while ψ_α and $\bar{\psi}_\alpha$ ($\alpha = 1, \ldots, 4$) are $N \times N$ traceless matrices with Grassmannian entries. The scale parameter g can be absorbed by an appropriate rescaling of the matrices, and we set $g^2 N = 1$ without loss of generality. Then the actions become

$$S_\mathrm{b} = -\frac{1}{4} N \mathrm{tr} \, [A_\mu, A_\nu]^2 \ , \tag{2.2}$$

$$S_\mathrm{f} = -\frac{1}{2} N \mathrm{tr} \, \left(\bar{\psi}_\alpha (\Gamma_\mu)_{\alpha\beta} [A_\mu, \psi_\beta] \right) \ . \tag{2.3}$$

The integration measure is given by

$$dA = \prod_{a=1}^{N^2-1} \prod_{\mu=1}^{6} \frac{dA_\mu^a}{\sqrt{2\pi}} \ ,$$

$$d\psi d\bar{\psi} = \prod_{a=1}^{N^2-1} \prod_{\alpha=1}^{4} d\psi_\alpha^a d\bar{\psi}_\alpha^a \ , \tag{2.4}$$

where $A_\mu = \sum_{a=1}^{N^2-1} A_\mu^a T^a$, $\psi_\alpha = \sum_{a=1}^{N^2-1} \psi_\alpha^a T^a$ and $\bar{\psi}_\alpha = \sum_{a=1}^{N^2-1} \bar{\psi}_\alpha^a T^a$. The $\mathrm{SU}(N)$ generators T^a are normalized so that $\mathrm{tr}(T^a T^b) = \frac{1}{2}\delta^{ab}$. The model has an SO(6) symmetry,

under which A_μ transform as a vector and ψ_α, $\bar\psi_\alpha$ as Weyl spinors, respectively. The gamma matrices after Weyl projection are 4×4 matrices, which we take to be

$$\Gamma_1 = \sigma_1 \otimes \sigma_2 \,, \quad \Gamma_2 = \sigma_2 \otimes \sigma_2 \,, \quad \Gamma_3 = \sigma_3 \otimes \sigma_2 \,,$$
$$\Gamma_4 = \mathbf{1} \otimes \sigma_1 \,, \quad \Gamma_5 = \mathbf{1} \otimes \sigma_3 \,, \quad \Gamma_6 = i\mathbf{1} \otimes \mathbf{1} \,. \tag{2.5}$$

The model (2.1) is formally obtained by the dimensional reduction of the $D = 6$, $\mathcal{N} = 1$, SU(N) super Yang-Mills theory. Similar reductions can be considered for $D = 3, 4$ and 10 dimensions, the last being the IIB matrix model [2]. The partition function (2.1) is potentially non-finite due to the non-compact measure and the flat directions $[A_\mu, A_\nu] = 0$ in the action. Quantum effects[3], however, render it finite for $D > 3$, a fact that has been checked both numerically [17] and analytically [18].

The model is studied by first integrating out the fermions, after which we obtain

$$Z = \int dA \, \mathrm{e}^{-S_\mathrm{b}[A]} \, Z_\mathrm{f}[A] \,, \tag{2.6}$$

where $Z_\mathrm{f}[A]$ represents the fermionic partition function defined by

$$Z_\mathrm{f}[A] = \int d\psi \, d\bar\psi \, \mathrm{e}^{-S_\mathrm{f}} = \det \mathcal{M}[A] \,. \tag{2.7}$$

The matrix $\mathcal{M}[A]$ is a $4(N^2-1) \times 4(N^2-1)$ matrix, whose explicit form is given by eq. (A.11) in appendix A. For a generic configuration, $\det \mathcal{M}[A] = |\det \mathcal{M}[A]|\mathrm{e}^{i\Gamma}$ is complex, and eq. (2.6) becomes

$$Z = \int dA \, \mathrm{e}^{-S_0[A]} \, \mathrm{e}^{i\Gamma[A]} \,, \tag{2.8}$$

where

$$S_0[A] = S_\mathrm{b}[A] - \log|\det \mathcal{M}[A]| \,. \tag{2.9}$$

The complex phase in eq. (2.8) is a common feature of the $D = 6, 10$ models, whereas for $D = 4$, we have $\Gamma[A] \equiv 0$. In the latter case, no SSB occurs [34, 36], consistent with the observation that the phase plays a central role in the SSB mechanism.

The properties of the phase relevant to the SSB were found in ref. [22], and numerical studies in ref. [23] confirmed the picture by showing that strong fluctuations of the phase are the main effect that suppresses symmetric configurations and favors non-symmetric ones despite their entropic suppression. First one notes that (i) configurations with $A_6 = 0$ give real[4] $\det \mathcal{M}[A]$, (ii) configurations with $A_5 = A_6 = 0$ give $\det \mathcal{M}[A] \geq 0$, and (iii) configurations with $A_3 = \ldots = A_6 = 0$ give $\det \mathcal{M}[A] \equiv 0$. Let us define "$d$-dimensional configurations" ($1 \leq d \leq 5$) as configurations of A_μ that can be transformed to $A_{d+1} = \ldots = A_6 = 0$ by an appropriate SO(6) transformation. Then, for $d \leq 4$, we have

$$\frac{\partial^k \Gamma[A]}{\partial A_{\mu_1} \ldots \partial A_{\mu_k}} = 0 \qquad \text{for} \qquad k = 1, \ldots, 6 - (d+1) \,. \tag{2.10}$$

---

[3]Naively one might think that quantum effects are canceled due to supersymmetry. In fact the flat direction is raised by quantum effects from fermion zero modes that appear in a diagonal bosonic background as was first recognized in ref. [3].

[4]In this case, the determinant is not necessarily positive, but it turns out that configurations with positive determinant dominate at large N.

This is because up to $6 - (d+1)$-th order of perturbation, the configuration remains 5-dimensional, and therefore $\det \mathcal{M}[A]$ remains real non-negative. Strictly speaking, eq. (2.10) does not hold for $d \leq 2$ since $\det \mathcal{M}[A] \equiv 0$ for such configurations, and the phase $\Gamma[A]$ becomes ill-defined.

In order to probe the SSB of SO(6) rotational symmetry, we study the "moment of inertia" tensor

$$T_{\mu\nu} = \frac{1}{N} \mathrm{tr}\, (A_\mu A_\nu) \tag{2.11}$$

and its real positive eigenvalues λ_n $(n = 1, \ldots, 6)$ ordered as

$$\lambda_1 \geq \lambda_2 \geq \ldots \geq \lambda_6 \ . \tag{2.12}$$

The vacuum expectation values (VEVs) $\langle \lambda_n \rangle$, taken *after* the ordering for each configuration, play the role of order parameters. If they turn out to be unequal in the large-N limit, it implies SSB of SO(6).

The VEVs $\langle \lambda_n \rangle$ have been calculated in the large-N limit by the GEM [51] for the SO(d) symmetric vacuum $(2 \leq d \leq 5)$, which has

$$\langle \lambda_1 \rangle_{\mathrm{SO}(d)} = \ldots = \langle \lambda_d \rangle_{\mathrm{SO}(d)} \equiv (R_d)^2 \tag{2.13}$$

due to the SO(d) symmetry. The small eigenvalues $\langle \lambda_k \rangle_{\mathrm{SO}(d)}$ with $k > d$ have little dependence on k for each d, and moreover the mean value turns out to be universal for all d. The results for $(R_d)^2$ $(3 \leq d \leq 5)$, on the other hand, are fitted nicely to[5]

$$(R_d)^d r^{6-d} = \ell^6 \tag{2.14}$$

with $r^2 \approx 0.223$ and $\ell^2 \approx 0.627$. The value of r^2 turns out to be consistent with the universal scale in the small directions. Therefore, the left-hand side of (2.14) actually represent the six-dimensional volume of the dynamical space-time, and hence eq. (2.14) is called the constant volume property. This implies that the dynamical space-time in this model behaves effectively as an incompressible fluid and that the phase of the fermion determinant can only make it collapsed without changing its volume. Physical understanding of the universal scale r and the constant volume property is discussed in section 6 of ref. [51] based on low-energy effective theory [3].

3   The complex-action problem and the factorization method

Monte Carlo calculations of $\langle \lambda_n \rangle$ are quite hard due to the strong fluctuations of the phase $\Gamma[A]$ in eq. (2.8). A straightforward approach is to simulate the phase-quenched model

$$Z_0 = \int dA \, \mathrm{e}^{-S_0[A]} \ , \tag{3.1}$$

---

[5]The GEM results for $d = 2$ do not satisfy this property, which may be due to the subtlety in the calculations for the $d = 2$ case explained in ref. [51].

and to compute VEVs in the full model by reweighting[6]

$$\langle \lambda_n \rangle = \frac{\langle \lambda_n \, e^{i\Gamma} \rangle_0}{\langle e^{i\Gamma} \rangle_0} = \frac{\langle \lambda_n \, \cos \Gamma \rangle_0}{\langle \cos \Gamma \rangle_0} \; , \tag{3.2}$$

where $\langle \cdot \rangle_0$ are VEVs taken with respect to the phase-quenched model in eq. (3.1). This approach suffers from the complex-action problem and the overlap problem. The VEVs $\langle \cdot \, e^{i\Gamma} \rangle_0$ decrease exponentially at large N as $e^{-N^2 \Delta F}$, where $\Delta F > 0$ is the difference of the free energies of the full and phase-quenched models defined by the ratio Z/Z_0. This happens via huge cancellations due to the oscillating terms from the phase factor $e^{i\Gamma}$. As a result, one needs $\mathcal{O}(e^{\text{const.} \times N^2})$ configurations to compute an observable with given accuracy. This is the complex-action problem or the sign problem. The overlap problem is due to the exponentially small overlap of the distribution of the configurations sampled in Z_0 with the important configurations in Z with increasing N.

In order to overcome the complex-action problem and the overlap problem, a new method termed the factorization method was proposed in refs. [23, 42]. We review the refined version [42] as applied to the present model.

In what follows, we study the normalized eigenvalues

$$\tilde{\lambda}_n = \frac{\lambda_n}{\langle \lambda_n \rangle_0} \; . \tag{3.3}$$

The deviation of $\langle \tilde{\lambda}_n \rangle$ from 1 represents the effect of the phase. We consider the distribution functions

$$\rho(x_1, \ldots, x_6) = \left\langle \prod_{k=1}^{6} \delta(x_k - \tilde{\lambda}_k) \right\rangle \tag{3.4}$$

$$\text{and} \quad \rho^{(0)}(x_1, \ldots, x_6) = \left\langle \prod_{k=1}^{6} \delta(x_k - \tilde{\lambda}_k) \right\rangle_0 \tag{3.5}$$

for the full model and the phase-quenched model, respectively. These functions vanish due to the ordering (2.12) unless[7] $x_1 \langle \lambda_1 \rangle_0 \geq \ldots \geq x_6 \langle \lambda_6 \rangle_0$. By applying the reweighting formula like (3.2) to the right-hand side of eq. (3.4), one finds that it factorizes as

$$\rho(x_1, \ldots, x_6) = \frac{1}{C} \, \rho^{(0)}(x_1, \ldots, x_6) \, w(x_1, \ldots, x_6) \; . \tag{3.6}$$

The function $w(x_1, \ldots, x_6)$ is defined by[8]

$$w(x_1, \ldots, x_6) = \langle e^{i\Gamma} \rangle_{x_1, \ldots, x_6} = \langle \cos \Gamma \rangle_{x_1, \ldots, x_6} \; , \tag{3.7}$$

---

[6]In the second equality, we have used the fact that in the phase-quenched model, the phase Γ flips sign under the parity transformation $A_6 \to -A_6$. Similar remarks apply to eqs. (3.7), (3.9) and (3.13) as well.

[7]In the large-N limit, $\langle \lambda_n \rangle_0$ approaches a constant independent of n (see figure 1), which implies that the condition becomes $x_1 \geq \ldots \geq x_6$.

[8]Numerically, this function is found to be positive, which simplifies our analysis considerably. See ref. [39] for an analysis of a system in which the corresponding function is complex.

where $\langle \cdot \rangle_{x_1,\ldots,x_6}$ denotes a VEV with respect to the partition function

$$Z_{x_1,\ldots,x_6} = \int dA \, \mathrm{e}^{-S_0[A]} \prod_{k=1}^{6} \delta(x_k - \tilde{\lambda}_k) \ . \tag{3.8}$$

The real parameter C is a normalization constant given by

$$C = \langle \mathrm{e}^{i\Gamma} \rangle_0 = \langle \cos\Gamma \rangle_0 \ , \tag{3.9}$$

which is *not* needed in the calculations using the factorization method.

The VEVs $\langle \tilde{\lambda}_n \rangle$ can be written in terms of the distribution function as

$$\langle \tilde{\lambda}_n \rangle = \int \prod_{k=1}^{6} dx_k \, x_n \, \rho(x_1,\ldots,x_6) \ . \tag{3.10}$$

In the large-N limit, the integral is dominated by the minimum of the "free energy"

$$\begin{aligned}
\mathcal{F}(x_1,\ldots,x_6) &= -\frac{1}{N^2} \log \rho(x_1,\ldots,x_6) \tag{3.11} \\
&= -\frac{1}{N^2} \log \rho^{(0)}(x_1,\ldots,x_6) - \frac{1}{N^2} \log w(x_1,\ldots,x_6) + \frac{1}{N^2} \log C \ .
\end{aligned}$$

In order to obtain the minimum, we solve a set of coupled equations

$$\frac{1}{N^2} \frac{\partial}{\partial x_n} \log \rho^{(0)}(x_1,\ldots,x_6) = -\frac{\partial}{\partial x_n} \frac{1}{N^2} \log w(x_1,\ldots,x_6) \quad \text{for} \quad n = 1,\ldots,6 \ , \tag{3.12}$$

where the function on each side has a definite large-N limit. In fact there are more than one solutions, and we need to identify the minimum eventually by comparing the free energy at each solution. This way we can get a robust estimate for the VEVs $\langle \tilde{\lambda}_n \rangle$, which becomes exact in the large-N limit. Although calculations of the right-hand side of eq. (3.12) still suffer from the fluctuations of the phase, the effect is greatly reduced for two reasons: For given N, the system is constrained in the region of configuration space favored by the competition of entropic effects, the real action and the phase fluctuations. In this region, phase fluctuations are greatly reduced compared to the region mainly sampled by the phase-quenched model. Furthermore, it is possible to extrapolate $\frac{1}{N^2} \log w(x_1,\ldots,x_6)$ to larger values of N than allowed by direct simulation [23].

In applications to general complex-action systems, finding the operators that are strongly correlated with the phase is crucial for the success of the method [42, 43]. The choice of the observables in the present model is due to the strong correlation of λ_n with the phase Γ as expected from the arguments below eq. (2.9). By solving eq. (3.12), one can determine the important configurations in eq. (2.8). It is then straightforward to do effective importance sampling by constraining the system in the region of the solutions. Thus the overlap problem is solved. The VEV of any other observable weakly correlated with the phase $\mathrm{e}^{i\Gamma}$ can be obtained by estimating them in the constrained system (3.8) at the solutions.

In practice, numerically solving eq. (3.12) in its full generality in the 6d parameter space $(x_1,\ldots,x_6)$ is a formidable task. In a simplified model studied in refs. [42, 43], we

reduced the task by assuming that some subgroup of the rotational symmetry is unbroken in each of possible vacua. Similarly, we would like to study the $\mathrm{SO}(d)$ symmetric vacua with $2 \leq d \leq 5$, which correspond to the solutions to eq. (3.12) with $x_1 = \ldots = x_d > 1 > x_{d+1}, \ldots, x_6$. In fact we can reduce the computational task further by noting that the effect of the phase in the present model is such that some of the eigenvalues λ_n become maximally small, and the others become quite large. The large eigenvalues, as far as they are sufficiently large, do not affect much the fluctuation of the phase as we will see later. Therefore we may omit the large eigenvalues from the set of observables to be constrained in the factorization method. The small eigenvalues, on the other hand, tend to acquire the same value[9] for entropic reasons. This allows us to constrain only λ_{d+1}, the largest eigenvalue among the small ones, when we study the $\mathrm{SO}(d)$ symmetric vacuum.[10]

Below we describe how we can estimate the VEVs $\langle \tilde{\lambda}_n \rangle_{\mathrm{SO}(d)}$ and the free energy $\mathcal{F}_{\mathrm{SO}(d)}$ for the $\mathrm{SO}(d)$ symmetric vacuum under the above assumptions. We define

$$w_n(x) = \langle e^{i\Gamma} \rangle_{n,x} = \langle \cos\Gamma \rangle_{n,x} \ , \tag{3.13}$$

where the VEV is taken with respect to the $\tilde{\lambda}_n$-constrained system

$$Z_{n,x} = \int dA \, e^{-S_0[A]} \, \delta(x - \tilde{\lambda}_n) \ . \tag{3.14}$$

We also define

$$\rho_n^{(0)}(x) = \left\langle \delta(x - \tilde{\lambda}_n) \right\rangle_0 \ . \tag{3.15}$$

Under the present assumptions, the problem reduces to finding a solution $\bar{x}_n$ to

$$\frac{1}{N^2} f_n^{(0)}(x) \equiv \frac{1}{N^2} \frac{d}{dx} \log \rho_n^{(0)}(x) = -\frac{d}{dx} \frac{1}{N^2} \log w_n(x) \tag{3.16}$$

in the $x < 1$ region. Then the solution $\bar{x}_n$ with $n = d+1$ gives an estimate for the small eigenvalue $\langle \tilde{\lambda}_{d+1} \rangle_{\mathrm{SO}(d)}$ in the $\mathrm{SO}(d)$ symmetric vacuum in the large-N limit. The other eigenvalues in the $\mathrm{SO}(d)$ symmetric vacuum can be estimated as

$$\langle \lambda_k \rangle_{\mathrm{SO}(d)} = \langle \lambda_k \rangle_{n,\bar{x}_n} \ , \quad \text{where } n = d+1 \ . \tag{3.17}$$

Free energy for the $\mathrm{SO}(d)$ symmetric vacuum is given by estimating (3.11) at the corresponding solution of eq. (3.12). Under the present assumptions, the free energy for the $\mathrm{SO}(d)$ symmetric vacuum can be estimated up to a common constant by

$$\mathcal{F}_{\mathrm{SO}(d)} = \int_{\bar{x}_n}^{1} \frac{1}{N^2} f_n^{(0)}(x) dx - \frac{1}{N^2} \log w_n(\bar{x}_n) \ , \quad \text{where } n = d+1 \ . \tag{3.18}$$

By comparing the free energy for different d, we can determine the true vacuum, which gives the minimum of the free energy (3.11). The other vacua actually correspond to the saddle-points of the free energy (3.11).

---

[9]This property has been observed in the GEM calculations [51] as we mentioned below eq. (2.13).

[10]After this simplification, our task reduces *formally* to that of the single-observable factorization method, as originally proposed in ref. [23]. However, we emphasize that the interpretation we adopt in this work is based on the multi-observable factorization method [42] described above, and it is different from the one in ref. [23]. For instance, the overlap problem may occur when we calculate (3.13) by simulating the system (3.14) as pointed out in ref. [43]. This is not a problem, though, when we interpret the solution to (3.16) in the $x < 1$ region as an estimate of $\langle \tilde{\lambda}_{d+1} \rangle_{\mathrm{SO}(d)}$ for $n = d+1$.

4 Simulations and the results

Monte Carlo simulations are performed on the system

$$Z_{n,V} = \int dA \, e^{-S_0[A] - V(\lambda_n[A])} \ , \quad V(z) = \frac{1}{2} \gamma \, (z - \xi)^2 \ , \tag{4.1}$$

where γ and ξ are real parameters. For γ large enough, the Gaussian function approximates the delta function in eq. (3.14). We use the Rational Hybrid Monte Carlo (RHMC) algorithm [53] and the details of the simulations are described in appendix A.

The distribution functions of $\tilde{\lambda}_n$ for the system $Z_{n,V}$ are given by

$$\rho_{n,V}(x) \equiv \left\langle \delta(x - \tilde{\lambda}_n) \right\rangle_{n,V} \propto \rho_n^{(0)}(x) \exp \left\{ -V \left(x \, \langle \lambda_n \rangle_0 \right) \right\} \ , \tag{4.2}$$

where $\langle \, \cdot \, \rangle_{n,V}$ represents a VEV with respect to $Z_{n,V}$. The position of the peak, which we denote by x_{p}, can be obtained by solving

$$0 = \frac{d}{dx} \log \rho_{n,V}(x) = f_n^{(0)}(x) - \langle \lambda_n \rangle_0 \, V' \left(x \, \langle \lambda_n \rangle_0 \right) \ . \tag{4.3}$$

For sufficiently large γ, the distribution function $\rho_{n,V}(x)$ is sharply peaked at x_{p} and we can use the VEV of $\tilde{\lambda}_n$ as an estimator for x_{p}, i.e.,

$$x_{\mathrm{p}} = \langle \tilde{\lambda}_n \rangle_{n,V} \ . \tag{4.4}$$

By varying the value of ξ in eq. (4.1), we obtain the functions $w_n(x)$ and $f_n^{(0)}(x)$ by

$$w_n(x_{\mathrm{p}}) = \langle \cos \Gamma \rangle_{n,V} \ , \tag{4.5}$$

$$f_n^{(0)}(x_{\mathrm{p}}) = \langle \lambda_n \rangle_0 \, V' \left(\langle \lambda_n \rangle_{n,V} \right) = \gamma \langle \lambda_n \rangle_0 \left(\langle \lambda_n \rangle_{n,V} - \xi \right) \ . \tag{4.6}$$

The parameter γ should be chosen large enough to make the fluctuation of $\tilde{\lambda}_n$ smaller than the required resolution in x. It should not be too large because in that case, $(\langle \lambda_n \rangle_{n,V} - \xi) \propto 1/\gamma$, and a small error in $\langle \lambda_n \rangle_{n,V}$ propagates to $f_n^{(0)}(x)$ by a factor of γ. In practice, one makes sure that the results for a given value of x are independent of the choice of (γ, ξ) up to the accuracy goal[11]. This method of computing $f_n^{(0)}(x)$ is quite different from a direct computation of the distribution $\rho_n^{(0)}(x)$ of $\tilde{\lambda}_n$ in the phase-quenched model Z_0, where one can obtain reasonable statistics only in the vicinity of the peak $x = 1$. In contrast, our method enables us to measure in regions of configuration space suppressed by many orders of magnitude.

The phase-quenched model Z_0 corresponds to the special case $\gamma = 0$ of eq. (4.1). We simulate this system and compute $\langle \lambda_n \rangle_0$, $n = 1, \ldots, 6$, the results of which are shown in figure 1. We find that the data can be nicely fitted to $\langle \lambda_n \rangle_0 = c + \mathcal{O}(1/N)$, where c is chosen to be $\ell^2 = 0.627$, which appears in the constant volume property (2.14) obtained by the GEM. (This agreement $c = \ell^2$ is consistent with the physical interpretation of the constant

---

[11]Typically we use $\gamma \sim 100 - 1000$, but we have tested values up to $\gamma \sim 10^6$ and verified that the results are independent of γ.
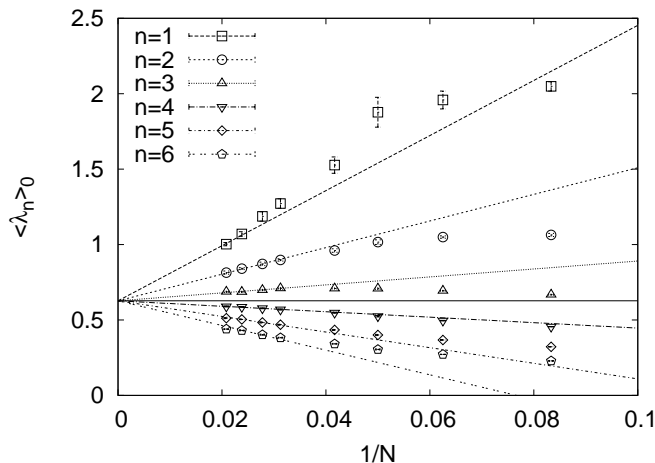
Figure 1. The eigenvalues $\langle\lambda_n\rangle_0$ for the phase-quenched model are plotted against $1/N$. The solid line represents the value $\ell^2 = 0.627$, which appears in eq. (2.14) obtained by the GEM [51]. The other lines represent the fits to the behavior $\langle\lambda_n\rangle_0 = \ell^2 + \mathcal{O}(1/N)$.

volume property given below eq. (2.14).) Thus the absence of a fluctuating phase results in no SSB of SO(6) as expected [33–36]. We should also note that finite-N effects make the eigenvalues $\langle\lambda_n\rangle_0$ depend much on n. The normalization (3.3) is useful in reducing such finite-N effects and making it easier to see the large-N scaling behavior in the following analysis.

Computing $w_n(x)$ using eq. (4.5) is hard due to the complex-action problem, especially near $x \approx 1$. The computation is easier in the region near the solution to eq. (3.16), where the fluctuations of the phase are milder. In such a region, one can make a sensible large-N extrapolation of

$$\Phi_n(x) = \lim_{N\to\infty} \frac{1}{N^2} \log w_n(x) \ . \tag{4.7}$$

The above scaling is observed in figure 2, where we show our results for $\frac{1}{N^2} \log w_n(x)$ with $n = 3, 4, 5, 6$ and $N = 12, 24$. The quality of convergence is similar to the oneloop model studied in ref. [23] and the model studied in refs. [42, 43]. We also have data for other N with less statistics, which confirm the observed scaling behavior further. Then one can use the equation

$$\frac{1}{N^2} f_n^{(0)}(x) = -\frac{d}{dx} \Phi_n(x) \tag{4.8}$$

in order to obtain the solution $\bar{x}_n(< 1)$ to (3.16) in the large-N limit. The left-hand side of the above equation can be calculated without the complex-action problem, and therefore we can obtain results at values of N larger than the ones used in order to determine $\Phi_n(x)$. This feature of the factorization method turns out to be crucial in the present work since $\frac{1}{N^2} f_n^{(0)}(x)$ suffers from severe finite-N effects in the interesting region of x as we will see.

The function $\Phi_n(x)$ has an asymptotic behavior in the $x \ll 1$ region that can be easily understood geometrically [43]. Note first that the dominant configurations in the ensemble (3.14) for $x \ll 1$ have $(7 - n)$ shrunken directions and they are approximately $d = (n - 1)$

n	$a_n \times 10^2$	$b_n \times 10^3$	c_n	d_n	p_n	q_n
3	24(2)	1.21(7)	$-2.7(3)$	2.2(7)	2.2(1)	14.0(3)
4	5.0(5)	1.2(1)	$-3.4(6)$	0(1)	4.6(2)	15.5(2)
5	1.45(9)	1.34(7)	$-3.7(3)$	$-1.3(7)$	4.3(3)	17.9(4)
6	0.69(7)	1.0(2)	$-3.6(3)$	$-1.9(8)$	3.0(3)	16.4(7)

Table 1. The results for the fitting parameters are shown. The parameters a_n and b_n in (4.9) are obtained from figure 3. The parameters c_n and d_n in (4.12) are obtained from figure 4. The parameters p_n and q_n in (4.13) are obtained from figure 5.

dimensional. Since the phase of the determinant vanishes for collapsed configurations (see discussion that leads to eq. (2.10) and the footnote 4), $w_n(x) \equiv \langle e^{i\Gamma} \rangle_{n,x}$ is expected naively to approach 1 as $x \to 0$.

From figures 2 and 3, we find that $w_n(x)$ actually approaches a value slightly smaller than 1 as $x \to 0$. This can be understood intuitively as follows. As x becomes small, λ_k with $k = n, \ldots, 6$ become small, but λ_k with $k = 1, \ldots, (n-1)$ become large for entropic reasons. Then, due to the bosonic action S_b in eq. (2.2), the matrices A_μ tend to become simultaneously diagonal up to SU(N) symmetry. For such configurations, the fermionic action S_f has quasi-zero-modes corresponding to diagonal fermionic matrices, and the phase fluctuation of the fermion determinant is enhanced.[12] It is conceivable that this effect balances against the suppression of the phase fluctuation due to collapsing space-time, and leads to the small deviation from the expected asymptotic behavior.[13]

In fact, the asymptotic behavior of $w_n(x)$ for $x \ll 1$ can be fitted well to

$$\frac{1}{N^2} \log w_n(x) \simeq -a_n x^{7-n} - b_n \quad \text{for} \quad x \ll 1, \quad n = 2, 3, 4, 5, 6 \tag{4.9}$$

as shown in figure 3. The coefficients a_n and b_n obtained by the fits are given in table 1. The existence of a small positive constant b_n can be attributed to the effect just mentioned. The first power-law term in eq. (4.9) can be derived [43] from eq. (2.10), which implies that the fluctuation of the phase around a collapsed configuration with $1 \le d \le 5$ is of the order of $\delta\Gamma \sim (\delta A / |A|)^{6-d}$, where δA and $|A|$ represent a typical scale of A_μ in the shrunken and extended directions, respectively. From eq. (2.11) we expect that $\delta A / |A| \propto \sqrt{x}$ and that the width of the distribution of the phase is $\sigma \propto (\sqrt{x})^{7-n}$. Assuming that the distribution is Gaussian, the VEV of $e^{i\Gamma}$ is given by $\int d\Gamma \frac{1}{\sqrt{2\pi}\sigma} \exp\left(-\frac{1}{2\sigma^2}\Gamma^2\right) e^{i\Gamma} = \exp\left(-\frac{1}{2}\sigma^2\right)$, which gives $-\log w_n(x) = \frac{1}{2}\sigma^2 \propto x^{7-n}$.

Let us also comment on the large-x behavior of $w_n(x)$ although it is not of our primary interest in the present analysis since we are searching for solutions to eq. (3.16) in the $x < 1$ region. From figure 2, we find that $w_n(x)$ increases and approaches a constant at sufficiently

---

[12]For $n = 3$, we also have quasi-zero-modes associated with collapsed configurations with $d \le 2$, which increases the phase fluctuations as we mention below eq. (2.10).

[13]The small deviation from the geometric argument does not exist in the toy model studied in ref. [42, 43], which has a Gaussian action for the bosonic matrices instead of a commutator squared term (2.2). This is consistent with our intuitive explanation given here.
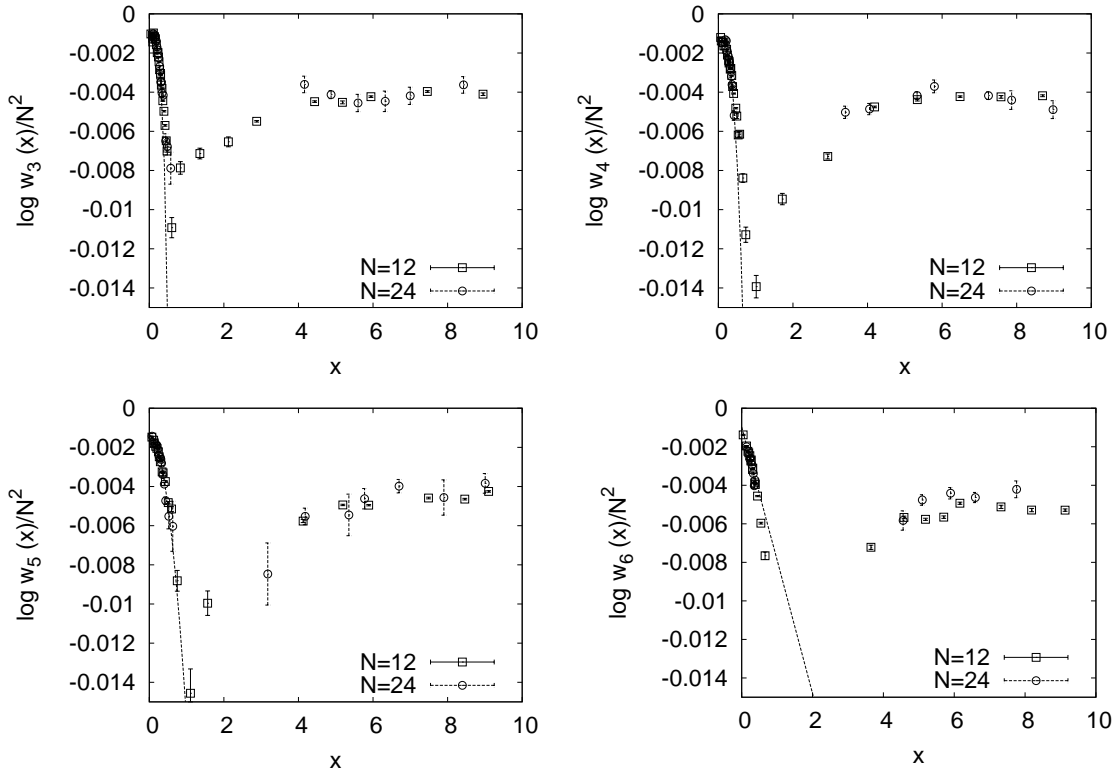
Figure 2. The function $\frac{1}{N^2} \log w_n(x)$ is plotted against x for $N = 12, 24$ with $n = 3, 4, 5, 6$. The dashed lines are the fits to the scaling ansatz (4.9) obtained in figure 3.

large x. This can be understood as follows. In the large-x regime, λ_k with $k = 1, \ldots, n$ are forced to be large, and due to the bosonic action S_{b} in eq. (2.2), the matrices A_μ tend to become simultaneously diagonal up to $\mathrm{SU}(N)$ symmetry. Then, neglecting the quasi-zero-modes discussed above eq. (4.9), the fermion determinant becomes positive definite[14]

$$\det \mathcal{M}[A] = \left[\prod_{i<j} (\alpha_{i\mu} - \alpha_{j\mu})^2 \right]^4 > 0 \, , \tag{4.10}$$

where $A_\mu = \mathrm{diag}(\alpha_{1\mu}, \ldots, \alpha_{N\mu})$. Due to the existence of the quasi-zero-modes, however, the VEV of $\mathrm{e}^{i\Gamma}$ becomes slightly below 1 for the same reason as before.[15] As a result, the dependence of $w_n(x)$ on x becomes quite mild in the large-x region. This leads to our assumption in section 3 that the large eigenvalues λ_n do not affect much the fluctuations of the phase.

---

[14]For $n \leq 5$, the dominant configuration in the large-x regime is n-dimensional, which adds to the suppression of the phase fluctuation. This effect is expected to become stronger for smaller n, which is seen in the behavior of $\frac{1}{N^2} \log w_n(x)$ as x decreases towards $x = 1$ in figure 2.

[15]Figure 2 shows that the constant value to which $w_n(x)$ approaches at large x depends very little on n. This is understandable since the value is determined by the dynamics of the quasi-zero modes represented by diagonal fermionic matrices, where the dimensionality of configurations does not play important roles.
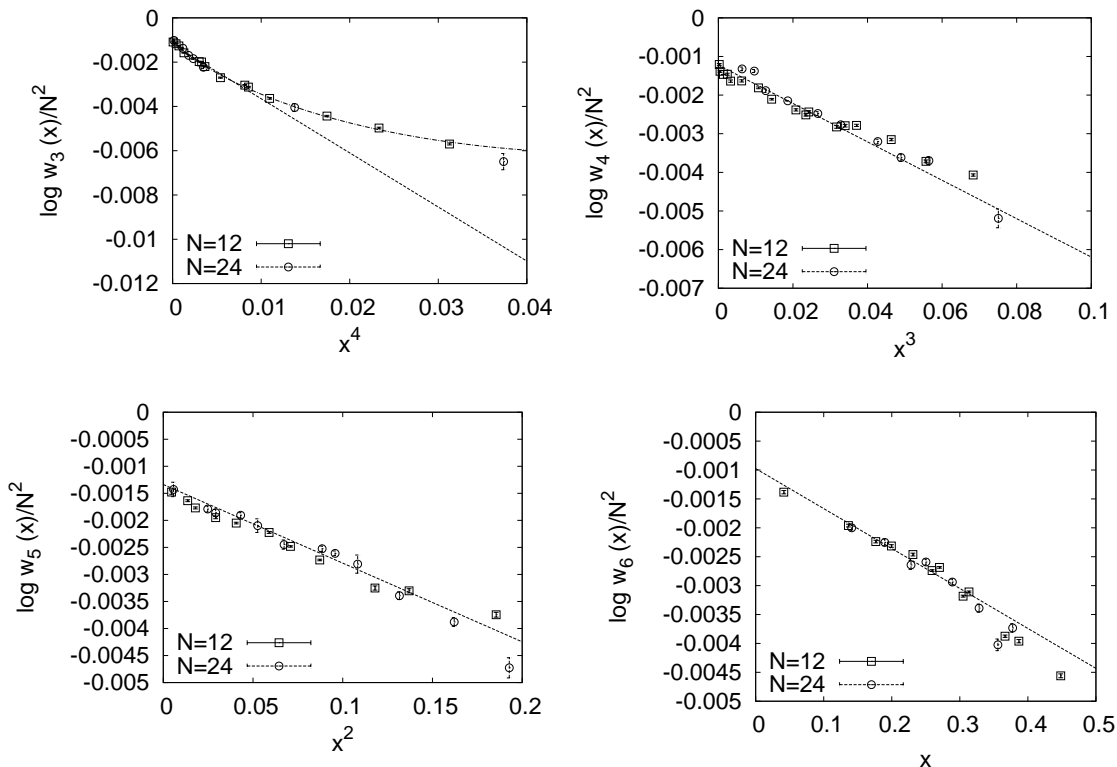
Figure 3. The function $\frac{1}{N^2}\log w_n(x)$ is plotted against x^{7-n} for $N = 12, 24$ with $n = 3, 4, 5, 6$. The dashed lines represent the fits of the $N = 24$ data to the scaling ansatz (4.9), which are used to compute $\Phi_n(x)$ in eq. (4.7). The dash-dotted line in the top-left panel represents a fit including a subleading term; See footnote 19.

Let us move on to the computation of the left-hand side of eq. (4.8). First we note that the small-x behavior of the function $\frac{1}{N^2}f_n^{(0)}(x)$ is expected to be[16]

$$\lim_{N\to\infty}\frac{1}{N^2}f_n^{(0)}(x)\simeq\frac{7-n}{2x}\ . \tag{4.11}$$

This can be understood [42, 43] in terms of the "phase-space suppression" since $(7-n)$ directions shrink as x becomes small. Each direction has an extent $\sim\sqrt{x}$, which results in $\rho_n^{(0)}(x)\sim(\sqrt{x})^{(7-n)(N^2-1)}$. From the definition (3.16) of $f_n^{(0)}(x)$, we obtain eq. (4.11).

In the region $x\gtrsim 0.4$, however, we find a completely different large-N scaling as shown in figure 4. It is actually $\frac{1}{N}f_n^{(0)}(x)$ that scales, which implies that $\frac{1}{N^2}f_n^{(0)}(x)$ vanishes as $\mathcal{O}(\frac{1}{N})$ in this region.[17] This can be understood as a result of cancellations by

---

[16]In the $n = 1$ case, which we do not study here, we have to consider that the eigenvalues of A_μ collapse to 0 for $x \ll 1$, and the suppression factor comes also from the fermion determinant, which is a homogeneous polynomial of A_μ of degree $4(N^2 - 1)$. This gives an extra suppression factor of $(\sqrt{x})^{4(N^2-1)}$. Hence eq. (4.11) should be replaced by $\lim_{N\to\infty}\frac{1}{N^2}f_1^{(0)}(x)\simeq\frac{5}{x}$.

[17]This reduction in the values of $\frac{1}{N^2}f_n^{(0)}(x)$ is not observed in the matrix model studied in ref. [42, 43], which has no supersymmetry.
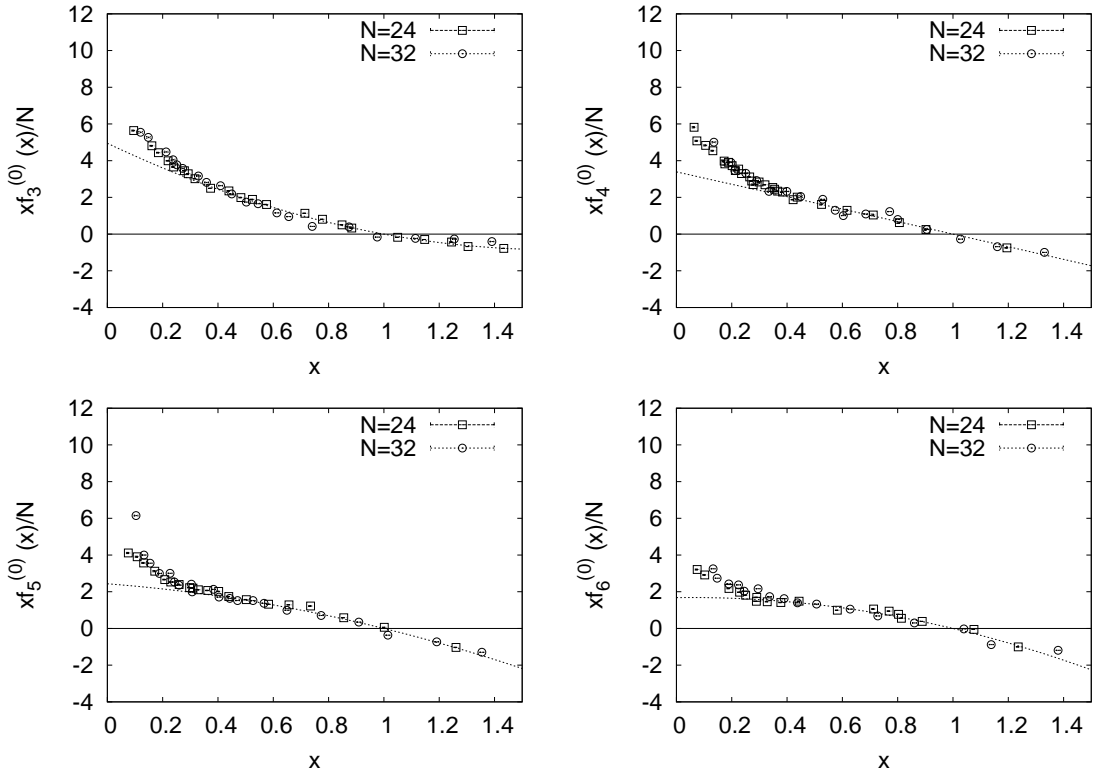
Figure 4. The function $\frac{x}{N} f_n^{(0)}(x)$ is plotted against x for $N = 24, 32$ with $n = 3, 4, 5, 6$. The dotted lines represent the fits of all the data within $0.4 \leq x \leq 1$ to the function $g_n(x)$ in eq. (4.12).

fermionic and bosonic contributions to the interactions among space-time points[18] as was first noted in the oneloop approximated model studied in ref. [23]. In that model, however, the $\frac{1}{N} f_n^{(0)}(x)$ scaling was observed also in the small-x region. This shows that the non-vanishing $\frac{1}{N^2} f_n^{(0)}(x)$ with the small-x behavior (4.11) arises in the full model considered here due to the small distance interactions of the eigenvalues, which are ignored in the oneloop model.

The existence of the $\mathcal{O}(\frac{1}{N})$ terms in $\frac{1}{N^2} f_n^{(0)}(x)$ obscures the leading large-N behavior, and a direct large-N extrapolation would require much larger N than we can study. Therefore we attempt to subtract the $\mathcal{O}(\frac{1}{N})$ terms in the following way. From figure 4 we find that the data for $\frac{1}{N} f_n^{(0)}(x)$ within $0.4 \leq x \leq 1$ can be fitted nicely to

$$\frac{x}{N} f_n^{(0)}(x) \simeq g_n(x) = c_n(x - 1) + d_n(x - 1)^2 , \qquad (4.12)$$

which implies a near Gaussian behavior of $\rho_n^{(0)}(x)$ around $x = 1$. The coefficients c_n and d_n

---

[18]The remaining $\mathcal{O}(\frac{1}{N})$ terms in $\frac{1}{N^2} f_n^{(0)}(x)$ can be attributed to the branched-polymer-like interaction [3] among the space-time points, which arises from the integration over the fermionic zero modes with only $\mathcal{O}(N)$ degrees of freedom. See also footnote 3.
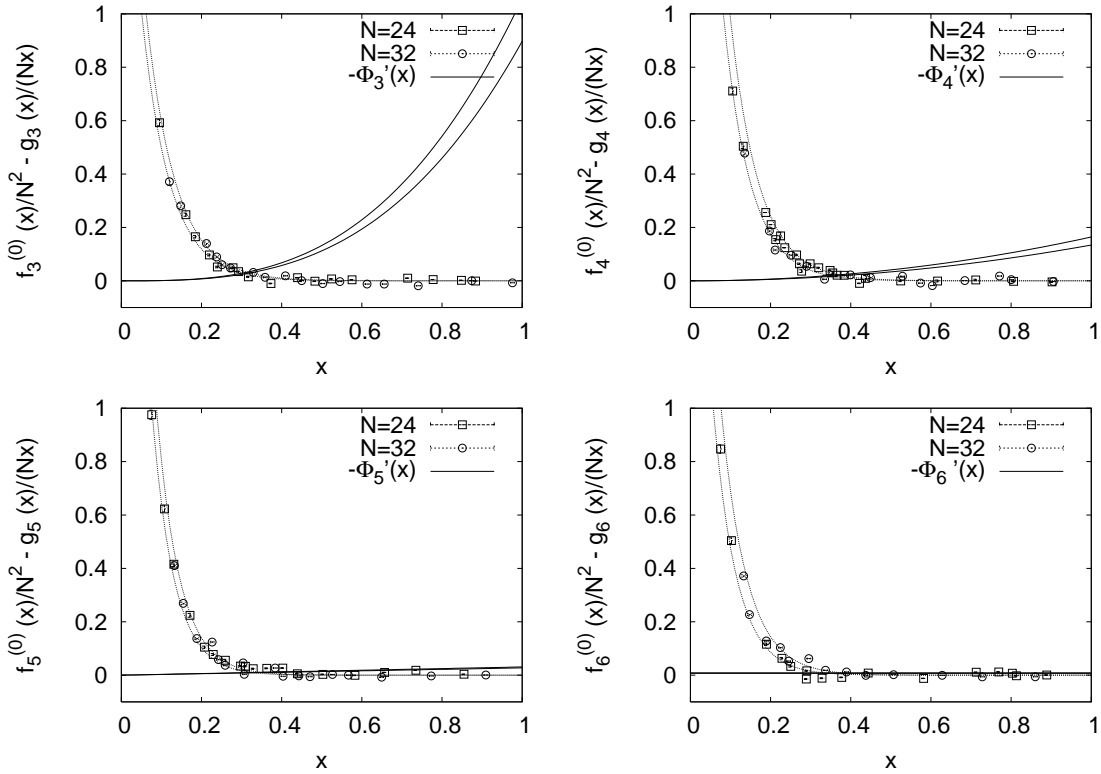
Figure 5. The function $\frac{1}{N^2}f_n^{(0)}(x) - \frac{g_n(x)}{Nx}$ is plotted against x for $N = 24, 32$ with $n = 3, 4, 5, 6$. The dotted lines represent the fits of all the data within $0.1 \leq x \leq 0.4$ to the ansatz (4.13). The solution to eq. (4.8) is then given by the intersection with the function $-\Phi'_n(x)$ represented by the solid lines with a margin.

obtained by the fits are given in table 1. We subtract the $\mathcal{O}(\frac{1}{N})$ terms in $\frac{1}{N^2}f_n^{(0)}(x)$ given by eq. (4.12) from our data, and show the results in figure 5. We find that the results for $N = 24$ and $N = 32$ scale reasonably well, and the data within $0.1 \leq x \leq 0.4$ can be fitted to a simple ansatz

$$\frac{1}{N^2}f_n^{(0)}(x) - \frac{g_n(x)}{Nx} = p_n \exp\left(-q_n x\right) \tag{4.13}$$

as shown in figure 5. The parameters p_n and q_n obtained by the fits are given in table 1.

In the same figure we also plot $-\Phi'_n(x)$, where we use eq. (4.9) with a_n and b_n shown in table 1 as an estimate of $\Phi_n(x)$. The values of x at the intersections with the function (4.13) are given as[19]

$$\bar{x}_3 = 0.33(1) \; , \quad \bar{x}_4 = 0.35(1) \; , \quad \bar{x}_5 = 0.34(2) \; , \quad \bar{x}_6 = 0.36(3) \; . \tag{4.14}$$

These values of $\bar{x}_n$ with $n = d+1$ provide estimates for $\langle \tilde{\lambda}_{d+1} \rangle_{\mathrm{SO}(d)}$ in the SO(d) symmetric vacua as explained below eq. (3.16). Recalling the adopted normalization (3.3) and our

---

[19]The value of $\bar{x}_3$ quoted here is obtained by taking into account the deviation of $\frac{1}{N^2}\log w_3(x)$ from the asymptotic behavior (4.9) at $x \gtrsim 0.3$ seen in the top-left panel of figure 3. As an estimate of $\Phi_3(x)$, we have actually used the dash-dotted line in the same panel, which represents a fit including a subleading term $\propto x^{9/2}$ [43]. If we use instead the dashed line representing a fit to (4.9), we obtain $\bar{x}_3 = 0.31(1)$.
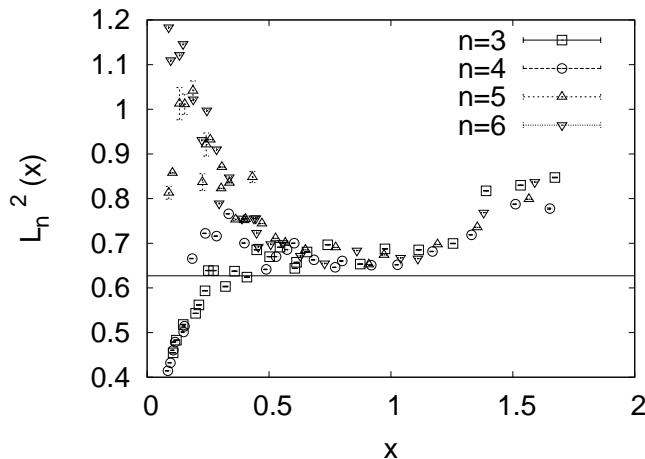
Figure 6. The geometric mean $L_n^2(x) = \left(\prod_{k=1}^6 \langle\lambda_k\rangle_{n,x}\right)^{\frac{1}{6}}$ is plotted for $N = 32$ with $n = 3, 4, 5, 6$. The solid line represents $\ell^2 = 0.627$, which appears in eq. (2.14) obtained by the GEM [51].

observation $\lim_{N\to\infty}\langle\lambda_n\rangle_0 = \ell^2$ from figure 1, we find that our results for $\langle\tilde{\lambda}_{d+1}\rangle_{\mathrm{SO}(d)}$ are in good agreement with

$$\langle\tilde{\lambda}_{d+1}\rangle_{\mathrm{SO}(d)} \equiv \frac{\langle\lambda_{d+1}\rangle_{\mathrm{SO}(d)}}{\langle\lambda_{d+1}\rangle_0} = \frac{r^2}{\ell^2} \approx \frac{0.223}{0.627} = 0.355 \; , \tag{4.15}$$

where we used the GEM predictions [51] reviewed at the end of section 2. Thus our results are consistent with the universal scale of small dimensions for all the $\mathrm{SO}(d)$ symmetric vacua with $2 \le d \le 5$.

Let us turn to the calculation of the large eigenvalues. The eigenvalues λ_k in the $\mathrm{SO}(d)$ symmetric vacua can be estimated by eq. (3.17). More generally, we consider $\langle\lambda_k\rangle_{n,x}$ for various x, and calculate them by

$$\langle\lambda_k\rangle_{n,x_{\mathrm{p}}} = \langle\lambda_k\rangle_{n,V} \; , \tag{4.16}$$

where the right-hand side can be measured in the system (4.1), and x_{p} on the left-hand side is defined by eq. (4.4). In particular, we calculate the geometric mean

$$L_n^2(x) = \left(\prod_{k=1}^6 \langle\lambda_k\rangle_{n,x}\right)^{\frac{1}{6}} \; . \tag{4.17}$$

The results are shown in figure 6, where we see that $L_n^2(x) \approx \ell^2 \approx 0.627$ within $0.5 < x < 1$ for all n, which is consistent with the implication of the constant volume property (2.14) discussed at the end of section 2. Let us note that, for $x = 1$, the system essentially becomes the phase-quenched model without any constraint, and therefore we have $\langle\lambda_k\rangle_{n,x=1} \approx \langle\lambda_k\rangle_0$ for all n. In view of the results in figure 1, the deviation of $L_n^2(x = 1)$ from ℓ^2 can be attributed to finite-N effects. Eq. (2.14) for the $\mathrm{SO}(d)$ symmetric vacua with $3 \le d \le 5$ suggests that the constant volume property extends to smaller x including $\bar{x}_n \approx 0.355$ for $4 \le n \le 6$. This is not clearly seen in figure 6 presumably due to finite-N effects, however.
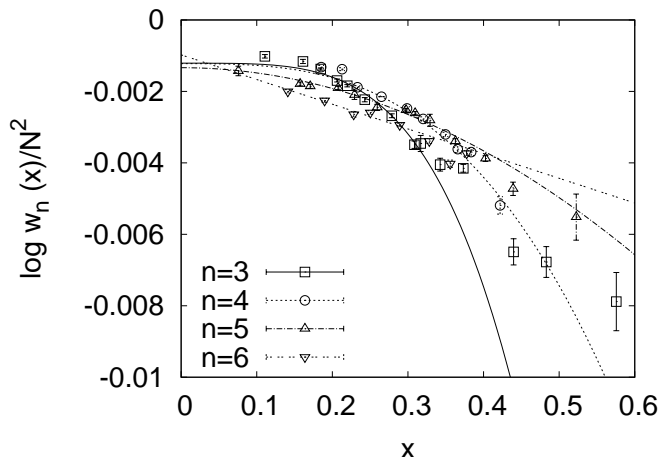
Figure 7. The function $\frac{1}{N^2} \log w_n(x)$ with $n = 3, 4, 5, 6$ are plotted together for $N = 24$.

Finally, we attempt to compare the free energies for the SO(d) vacua ($d = 2, 3, 4, 5$) using eq. (3.18). For simplicity, let us assume that $\bar{x}_n = 0.355$ as suggested by the GEM. The first term in eq. (3.18) can be estimated as

$$\int_{\bar{x}_n}^1 \frac{1}{N^2} f_n^{(0)}(x) dx = \frac{p_n}{q_n} (\mathrm{e}^{-q_n \bar{x}_n} - \mathrm{e}^{-q_n}) , \qquad (4.18)$$

where we have used the right-hand side of eq. (4.13) as an estimate for the large-N limit of $\frac{1}{N^2} f_n^{(0)}(x)$. Plugging in the values of p_n and q_n given in table 1, eq. (4.18) is estimated as 0.001, 0.001, 0.0004, 0.0005 for $n = 3, 4, 5, 6$, respectively. Next we discuss the second term in eq. (3.18). Figure 7 shows $\frac{1}{N^2} \log w_n(x)$ as a function of x for $N = 24$. We find that the values at $x = 0.355$ for $n = 3, 4, 5, 6$ differ at most by 0.001. Thus the results for $\mathcal{F}_{\mathrm{SO}(d)}$ with $d = 2, 3, 4, 5$ are quite close to each other. While our results do not contradict with an SO(3) symmetric true vacuum as predicted by the GEM [51], it seems difficult to determine the true vacuum only from our data.

5 Summary and discussions

We have performed Monte Carlo studies of a Euclidean six-dimensional version of the IIB matrix model, which is conjectured to be a nonperturbative definition of superstring theory. This model was studied before in the oneloop approximation, where the computational effort is $\mathcal{O}(N^2)$ smaller [23]. The simulation of the full model was made feasible by using state-of-the-art algorithms applied in recent studies of lattice QCD with dynamical fermions. A strong complex-action problem makes calculations very hard, and the factorization method was used in order to simulate the system efficiently in the region favored by the competing effects of the fluctuating phase, the real part of the action and the density of states. The maximum and the saddle-points of the distribution function for the eigenvalues λ_n of the tensor $T_{\mu\nu}$ were numerically computed by solving the equations (3.16), and the VEVs $\langle \lambda_n \rangle$ were estimated for SO(d) symmetric vacua. The large-N scaling properties

of the factorized distribution functions allowed efficient extrapolations of the functions to large N, which played an important role in the calculations.

The main goal of this work was to study, from first principles, the scenario for the dynamical compactification of space-time via SSB of SO(6) yielding SO(d) symmetric vacua with $d \leq 5$. The GEM calculations in ref.[51] provided strong support for this scenario by showing that the SO(3) symmetric vacuum has the lowest free energy. Moreover, the GEM predicted that the SO(d) symmetric vacua are characterized by a universal length scale r for the compactified dimensions, and that the length scale R_d for the large dimensions satisfies $(R_d)^d r^{6-d} = \ell^6$ with some dynamical constant ℓ, which may be understood as the constant volume property of the system. Our results are consistent with these predictions. First we find that the eigenvalues $\langle \lambda_n \rangle_0$ in the phase-quenched model, which does not have SSB, coincide in the large-N limit with the value of ℓ^2 obtained by the GEM. Second we obtain a d independent ($2 \leq d \leq 5$) value of r consistent with the numerical value given by the GEM. Third our results for the large dimensions are consistent with the constant volume property. We have confirmed the dramatic role of the fluctuations of the phase Γ by showing the absence of SSB in the phase-quenched model and the effect of $w_n(x)$ in generating dynamically the scale r instead of ℓ of the phase-quenched model. In actual determination of r, a crucial role is played by the hard core potential generated by the nonperturbative short distance dynamics of the eigenvalues, which was invisible in the oneloop approximation used in ref. [23].

We have also attempted to compare the free energy for SO(d) symmetric vacua ($2 \leq d \leq 5$). Although the comparison turned out to be subtle, we feel that the overall consistency between our results and the GEM calculations suggests that the conclusion obtained by the GEM [51] is correct. In the case of ten-dimensional IIB matrix model, the GEM [21] predicts that SSB of SO(10) also occurs, giving an SO(3) symmetric vacuum with three large dimensions. The physical interpretation of this statement requires special care, however, especially in the light of the recent results in ref.[24], where a $(3+1)$-dimensional *expanding* universe is found to arise dynamically in the *Lorentzian* IIB matrix model.

Last but not the least, we consider that our analysis demonstrates how the factorization method can be used in understanding nonperturbative dynamics of a complex-action system by Monte Carlo simulations. In particular, it is very encouraging that the method enabled us to study a physically interesting system in spite of the severe complex-action problem. Since the basic idea is quite general, we hope that the method can be applied to various interesting systems which are otherwise difficult to study.

Acknowledgments

A   Details of the Monte Carlo simulation

In this appendix we describe the details of the algorithm used in the Monte Carlo simulations of the system (4.1), where S_0 is given by (2.9). First we define the matrix $\mathcal{D} = \mathcal{M}^\dagger \mathcal{M}$ so that $|\det \mathcal{M}| = \det \mathcal{D}^{1/2}$. In the Rational Hybrid Monte Carlo (RHMC) algorithm [53], we use the rational approximation

$$x^{-1/2} \simeq a_0 + \sum_{k=1}^{Q} \frac{a_k}{x + b_k} \ , \tag{A.1}$$

where Q is chosen so that the error is small enough within the range of x required by the simulation. The real positive parameters a_k and b_k can be obtained by the code in ref. [54] using the Remez algorithm. Then it is possible to approximate $\det \mathcal{D}^{1/2}$ as

$$\det \mathcal{D}^{1/2} \simeq \int dF dF^* \, e^{-S_{\mathrm{PF}}[F,F^*,A]} \ , \tag{A.2}$$

$$\text{where} \quad S_{\mathrm{PF}}[F, F^*, A] = \mathrm{tr}\left\{ a_0 F^\dagger F + \sum_{k=1}^{Q} a_k F^\dagger \left(\mathcal{D} + b_k\right)^{-1} F \right\} \ , \tag{A.3}$$

and $(F_\alpha)_{ij}$ are auxiliary complex variables called pseudofermions. The range of the spectrum of $\mathcal{D}$ determines the accuracy goal in eq. (A.1).

In order to generate configurations, we use the Hybrid Monte Carlo method with the "Hamiltonian" H, which evolves the system in the fictitious time τ, where

$$H = \frac{1}{2}\mathrm{tr}\Pi^2 + \mathrm{tr}\tilde{\Pi}^\dagger\tilde{\Pi} + S_{\mathrm{eff}}[F, F^*, A] \ , \tag{A.4}$$

$$\text{and} \quad S_{\mathrm{eff}}[F, F^*, A] = S_{\mathrm{b}}[A] + S_{\mathrm{PF}}[F, F^*, A] + V(\lambda_n[A]) \ . \tag{A.5}$$

The auxiliary variables $\tilde{\Pi}_{ij}^\alpha$ and $\Pi_{ij}^\mu = (\Pi^*)_{ji}^\mu$ are defined to be canonical momenta of the $((F_\alpha)_{ij}, (A_\mu)_{ij})$ degrees of freedom so that $\int d\tilde{\Pi} d\tilde{\Pi}^* d\Pi dF dF^* dA \, e^{-H} = \int dF dF^* dA \, e^{-S_{\mathrm{eff}}}$ and that the equations of motion

$$\frac{dA_\mu}{d\tau} = \alpha \frac{\partial H}{\partial \Pi^\mu} = \alpha \Pi_\mu^* \ , \qquad \frac{dF_\beta}{d\tau} = \tilde{\alpha}\frac{\partial H}{\partial \tilde{\Pi}^\beta} = \tilde{\alpha}\tilde{\Pi}_\beta^* \ ,$$

$$\frac{d\Pi^\mu}{d\tau} = -\alpha \frac{\partial H}{\partial A_\mu} = -\alpha \frac{\partial S_{\mathrm{eff}}}{\partial A_\mu} \ , \qquad \frac{d\tilde{\Pi}^\beta}{d\tau} = -\tilde{\alpha}\frac{\partial H}{\partial F_\beta} = -\tilde{\alpha}\frac{\partial S_{\mathrm{eff}}}{\partial F_\beta} \ , \tag{A.6}$$

for the evolution in the fictitious time τ preserve the Hamiltonian H. The real coefficients α, $\tilde{\alpha}$ are Fourier acceleration coefficients [55], which, if optimized, can greatly reduce autocorrelation times. In our case we use $\alpha \simeq \frac{1}{6N^2}\langle \mathrm{tr}(A_\mu)^2\rangle$ and $\tilde{\alpha} \simeq \frac{1}{4N^2}\langle \mathrm{tr}(F_\beta)^2\rangle$.

This fictitious time-evolution is called the Molecular Dynamics. Numerically it is implemented by discretizing the equations of motion (A.6) with a time step $\Delta\tau$ and then integrating from $\tau = 0$ to $\tau = \tau_{\mathrm{f}}$ in N_τ steps, so that $\tau_{\mathrm{f}} = N_\tau \times \Delta\tau$. For that, the so-called leapfrog discretization is used in order to maintain time reversibility. The Hamiltonian H is now not conserved due to discretization errors and $\Delta H = H(\tau_{\mathrm{f}}) - H(0)$ is of $\mathcal{O}(\Delta\tau^2)$. A Metropolis accept/reject decision maintains detailed balance in order to obtain the correct distribution in the sampled configurations. The updating procedure therefore consists of the following steps:

- Refresh the momenta $(\tilde{\Pi}^\alpha(0), \Pi^\mu(0))$ according to their Gaussian $\mathrm{e}^{-\mathrm{tr}\tilde{\Pi}^\dagger\tilde{\Pi}}$, $\mathrm{e}^{-\frac{1}{2}\mathrm{tr}\Pi^2}$ distributions. This is necessary and sufficient for maintaining ergodicity.

- Evolve the $(\tilde{\Pi}^\alpha(0), \Pi^\mu(0), F_\alpha(0), A_\mu(0))$ configuration for time $\tau_{\mathrm{f}} = N_\tau \times \Delta\tau$ using the discretized versions of eq. (A.6).

- Accept or reject the $(F_\alpha(\tau_{\mathrm{f}}), A_\mu(\tau_{\mathrm{f}}))$ configuration with probability $\min(1, \mathrm{e}^{-\Delta H})$, where $\Delta H = H(\tau_{\mathrm{f}}) - H(0)$.

In the process, we have to keep τ_{f} large enough in order to reduce autocorrelation times and $\Delta\tau$ small enough in order to maintain reasonable acceptance rates. In practice, we first fix τ_{f} and optimize $\Delta\tau$ by maximizing $\Delta\tau \times (\text{acceptance rate})$. Then we optimize τ_{f} by minimizing autocorrelation times in units of Molecular Dynamics step. For more details, see ref. [35].

The main part of our computational effort is spent in the calculation of the terms containing $(\mathcal{D} + b_k)^{-1}F$, which appear in the Molecular Dynamics integration steps, as well as in the calculation of the Hamiltonian H. These terms are replaced by the solutions $(\chi_k)_{\alpha,ij}$ to the linear system $(\mathcal{D} + b_k)\chi_k = F$. For this we employ the conjugate gradient method for the smallest of the coefficients b_k and then use multimass Krylov solvers to compute the solutions for the other b_k [56]. This way we avoid $\mathcal{O}(Q)$ of arithmetic operations. The conjugate gradient method requires $\mathcal{O}(N^3)$ arithmetic operations[20] for each multiplication of χ_k by $\mathcal{M}$ [34]. The number of iterations for the convergence of the method is $\mathcal{O}(N^2)$, so each Molecular Dynamics step costs $\mathcal{O}(N^5)$. This is in contrast to the QCD case, where the conjugate gradient method converges after a number of iterations which is independent of the system size.

The term $\dfrac{\partial V(\lambda_n[A])}{\partial A_\mu}$, which appears in the left-bottom equation in (A.6), is calculated as follows. Using the relation

$$\sum_{\rho=1}^{6} T_{\nu\rho} v_\rho^{(n)} = \lambda_n v_\nu^{(n)}, \tag{A.7}$$

where $v_\mu^{(n)}$ ($n = 1, \ldots, 6$) are the six eigenvectors of the 6×6 matrix $T_{\mu\nu} = \dfrac{1}{N}\mathrm{tr}(A_\mu A_\nu)$ normalized as $\sum_{\mu=1}^{6} v_\mu^{(n)} v_\mu^{(n)} = 1$ for each n. Taking the derivative of eq. (A.7) with respect

---

[20]Naively one needs $\mathcal{O}(N^4)$ operations, but one notes that the nonzero elements in $\mathcal{M}$ are $\mathcal{O}(N^3)$. In actual calculation, we perform the multiplication of χ_k by $\mathcal{M}$ using the expression $\Gamma_\mu[A_\mu, \chi_k]$ as in ref. [34].

to $(A_\mu)_{kl}$, we obtain

$$\sum_{\rho=1}^{6} \left(\frac{\partial T_{\nu\rho}}{\partial(A_\mu)_{kl}} v_\rho^{(n)} + T_{\nu\rho} \frac{\partial v_\rho^{(n)}}{\partial(A_\mu)_{kl}} \right) = \frac{\partial \lambda_n}{\partial(A_\mu)_{kl}} v_\nu^{(n)} + \lambda_n \frac{\partial v_\nu^{(n)}}{\partial(A_\mu)_{kl}} \ . \tag{A.8}$$

Multiplying both sides of eq. (A.8) by $v_\nu^{(n)}$ and taking a sum over ν, we obtain

$$\sum_{\nu,\rho=1}^{6} v_\nu^{(n)} \frac{\partial T_{\nu\rho}}{\partial(A_\mu)_{kl}} v_\rho^{(n)} = \sum_{\nu=1}^{6} v_\nu^{(n)} \frac{\partial \lambda_n}{\partial(A_\mu)_{kl}} v_\nu^{(n)} = \frac{\partial \lambda_n}{\partial(A_\mu)_{kl}} \ , \tag{A.9}$$

where the second terms of each side of eq. (A.8) cancel. Therefore we obtain

$$\frac{\partial V(\lambda_n)}{\partial(A_\mu)_{kl}} = \gamma_n(\lambda_n - \xi_n) \frac{\partial \lambda_n}{\partial(A_\mu)_{kl}} = \frac{2\gamma_n}{N}(\lambda_n - \xi_n) \sum_{\nu=1}^{6} v_\mu^{(n)} v_\nu^{(n)} (A_\nu)_{lk} \ . \tag{A.10}$$

In order to calculate the phase of the fermion determinant, we calculate $\det\mathcal{M}[A]$ using (2.7) explicitly as described in ref. [34]. We define a complete basis of the general complex $N \times N$ matrices $t^a \in gl(N, \mathbb{C})$ by $(t^a)_{ij} = \delta_{ii_a}\delta_{jj_a}$, where $a = 1, \ldots, N^2$, $i_a, j_a = 1, \ldots, N$ and $a = N(i_a - 1) + j_a$. Taking into account the tracelessness of the fermionic matrices, the integration of $\psi, \bar\psi$ yields $\det\mathcal{M}[A]$, where the $4(N^2 - 1) \times 4(N^2 - 1)$ matrix $\mathcal{M}[A]$ is given by [34]

$$\mathcal{M}_{a\alpha,b\beta} = \mathcal{M}'_{a\alpha,b\beta} - \mathcal{M}'_{N^2\alpha,b\beta}\delta_{i_aj_a} - \mathcal{M}'_{a\alpha,N^2\beta}\delta_{i_bj_b} \ , \tag{A.11}$$

with $\alpha, \beta = 1, \ldots, 4$ and the $4N^2 \times 4N^2$ matrix $\mathcal{M}'$ defined by

$$\mathcal{M}'_{a\alpha,b\beta} = (\Gamma_\mu)_{\alpha\beta} \operatorname{tr}(t^a[A_\mu, t^b]) \ . \tag{A.12}$$

References

[1] J. Nishimura, *The origin of space-time as seen from matrix model simulations*, Prog. Theor. Exp. Phys. **2012** (2012) 01A101 [`arXiv:1205.6870`].

[2] N. Ishibashi, H. Kawai, Y. Kitazawa and A. Tsuchiya, *A large-N reduced model as superstring*, Nucl. Phys. **B 498** (1997) 467 [`hep-th/9612115`];
for a review, see e.g., H. Aoki, S. Iso, H. Kawai, Y. Kitazawa, A. Tsuchiya and T. Tada, *IIB matrix model*, Prog. Theor. Phys. Suppl. **134** (1999) 47 [`hep-th/9908038`];
T. Azuma, *Matrix models and the gravitational interaction*, `hep-th/0401120`.

[3] H. Aoki, S. Iso, H. Kawai, Y. Kitazawa and T. Tada, *Space-time structures from IIB matrix model*, Prog. Theor. Phys. **99** (1998) 713 [`hep-th/9802085`].

[4] J. M. Maldacena, *The Large N limit of superconformal field theories and supergravity*, Adv. Theor. Math. Phys. **2** (1998) 231 [`hep-th/9711200`].

[5] N. Itzhaki, J. M. Maldacena, J. Sonnenschein and S. Yankielowicz, *Supergravity and the large N limit of theories with sixteen supercharges*, Phys. Rev. **D 58** (1998) 046004 [`hep-th/9802042`].

[6] M. Hanada, J. Nishimura and S. Takeuchi, *Non-lattice simulation for supersymmetric gauge theories in one dimension*, Phys. Rev. Lett. **99** (2007) 161602 [`arXiv:0706.1647`].

[7] S. Catterall and T. Wiseman, *Towards lattice simulation of the gauge theory duals to black holes and hot strings*, *JHEP* **0712** (2007) 104 [`arXiv:0706.3518`].

[8] K. N. Anagnostopoulos, M. Hanada, J. Nishimura and S. Takeuchi, *Monte Carlo studies of supersymmetric matrix quantum mechanics with sixteen supercharges at finite temperature*, *Phys. Rev. Lett.* **100** (2008) 021601 [`arXiv:0707.4454`].

[9] S. Catterall and T. Wiseman, *Black hole thermodynamics from simulations of lattice Yang-Mills theory*, *Phys. Rev.* **D 78** (2008) 041502 [`arXiv:0803.4273`].

[10] M. Hanada, Y. Hyakutake, J. Nishimura and S. Takeuchi, *Higher derivative corrections to black hole thermodynamics from supersymmetric matrix quantum mechanics*, *Phys. Rev. Lett.* **102** (2009) 191602 [`arXiv:0811.3102`].

[11] S. Catterall and T. Wiseman, *Extracting black hole physics from the lattice*, *JHEP* **1004** (2010) 077 [`arXiv:0909.4947`].

[12] M. Hanada, A. Miwa, J. Nishimura and S. Takeuchi, *Schwarzschild radius from Monte Carlo calculation of the Wilson loop in supersymmetric matrix quantum mechanics*, *Phys. Rev. Lett.* **102** (2009) 181602 [`arXiv:0811.2081`].

[13] M. Hanada, J. Nishimura, Y. Sekino and T. Yoneya, *Monte Carlo studies of Matrix theory correlation functions*, *Phys. Rev. Lett.* **104** (2010) 151601 [`arXiv:0911.1623`].

[14] M. Hanada, J. Nishimura, Y. Sekino and T. Yoneya, *Direct test of the gauge-gravity correspondence for Matrix theory correlation functions*, *JHEP* **1112** (2011) 020 [`arXiv:1108.5153`].

[15] S. -J. Rey and J. -T. Yee, *Macroscopic strings as heavy quarks in large N gauge theory and anti-de Sitter supergravity*, *Eur. Phys. J.* **C 22** (2001) 379 [`hep-th/9803001`];
J. M. Maldacena, *Wilson loops in large N field theories*, *Phys. Rev. Lett.* **80** (1998) 4859 [`hep-th/9803002`];
S. -J. Rey, S. Theisen and J. -T. Yee, *Wilson-Polyakov loop at finite temperature in large N gauge theory and anti-de Sitter supergravity*, *Nucl. Phys.* **B 527** (1998) 171 [`hep-th/9803135`].

[16] Y. Sekino and T. Yoneya, *Generalized AdS-CFT correspondence for matrix theory in the large N limit*, *Nucl. Phys.* **B 570** (2000) 174 [`hep-th/9907029`].

[17] W. Krauth, H. Nicolai and M. Staudacher, *Monte Carlo approach to M-theory*, *Phys. Lett.* **B 431** (1998) 31 [`hep-th/9803117`];
W. Krauth and M. Staudacher, *Finite Yang-Mills integrals*, *Phys. Lett.* **B 435** (1998) 350 [`hep-th/9804199`].

[18] P. Austing and J. F. Wheater, *The Convergence of Yang-Mills integrals*, *JHEP* **0102** (2001) 028 [`hep-th/0101071`];
P. Austing and J. F. Wheater, *Convergent Yang-Mills matrix theories*, *JHEP* **0104** (2001) 019 [`hep-th/0103159`].

[19] J. Nishimura and F. Sugino, *Dynamical generation of four-dimensional space-time in the IIB matrix model*, *JHEP* **0205** (2002) 001 [`hep-th/0111102`].

[20] H. Kawai, S. Kawamoto, T. Kuroki, T. Matsuo and S. Shinohara, *Mean field approximation of IIB matrix model and emergence of four dimensional space-time*, *Nucl. Phys.* **B 647** (2002) 153 [`hep-th/0204240`];

H. Kawai, S. Kawamoto, T. Kuroki and S. Shinohara, *Improved perturbation theory and four-dimensional space-time in IIB matrix model*, *Prog. Theor. Phys.* **109** (2003) 115 [`hep-th/0211272`];
T. Aoyama and H. Kawai, *Higher order terms of improved mean field approximation for IIB matrix model and emergence of four-dimensional space-time*, *Prog. Theor. Phys.* **116** (2006) 405 [`hep-th/0603146`].

[21] J. Nishimura, T. Okubo and F. Sugino, *Systematic study of the SO(10) symmetry breaking vacua in the matrix model for type IIB superstrings*, *JHEP* **1110** (2011) 135 [`arXiv:1108.1293`].

[22] J. Nishimura and G. Vernizzi, *Spontaneous breakdown of Lorentz invariance in IIB matrix model*, *JHEP* **0004** (2000) 015 [`hep-th/0003223`];
J. Nishimura and G. Vernizzi, *Brane world generated dynamically from string type IIB matrices* *Phys. Rev. Lett.* **85** (2000) 4664 [`hep-th/0007022`].

[23] K. N. Anagnostopoulos and J. Nishimura, *New approach to the complex-action problem and its application to a nonperturbative study of superstring theory*, *Phys. Rev.* **D 66** (2002) 106008 [`hep-th/0108041`].

[24] S. -W. Kim, J. Nishimura and A. Tsuchiya, *Expanding (3+1)-dimensional universe from a Lorentzian matrix model for superstring theory in (9+1)-dimensions*, *Phys. Rev. Lett.* **108** (2012) 011601 [`arXiv:1108.1540`].

[25] H. Steinacker, *Split noncommutativity and compactified brane solutions in matrix models*, *Prog. Theor. Phys.* **126** (2011) 613 [`arXiv:1106.6153`].

[26] A. Chatzistavrakidis, *On Lie-algebraic solutions of the type IIB matrix model*, *Phys. Rev.* **D 84** (2011) 106010 [`arXiv:1108.1107`];
A. Polychronakos, H. Steinacker and J. Zahn, *Brane compactifications and 4-dimensional geometry in the IKKT model*, `arXiv:1302.3707`.

[27] S. -W. Kim, J. Nishimura and A. Tsuchiya, *Expanding universe as a classical solution in the Lorentzian matrix model for nonperturbative superstring theory*, *Phys. Rev.* **D 86** (2012) 027901 [`arXiv:1110.4803`].

[28] S. -W. Kim, J. Nishimura and A. Tsuchiya, *Late time behaviors of the expanding universe in the IIB matrix model*, *JHEP* **1210** (2012) 147 [`arXiv:1208.0711`].

[29] J. Nishimura and A. Tsuchiya, *Local field theory from the expanding universe at late times in the IIB matrix model*, *Prog. Theor. Exp. Phys.* **2013** (2013) 043B03 [`arXiv:1208.4910`].

[30] H. Aoki, *Chiral fermions and the standard model from the matrix model compactified on a torus*, *Prog. Theor. Phys.* **125** (2011) 521 [`arXiv:1011.1015`];
H. Aoki, *Probability of the standard model appearance from a matrix model*, *Phys. Rev.* **D 87** (2013) 046002 [`arXiv:1209.4514`];
H. Aoki, *Probability distribution over some phenomenological models in the matrix model compactified on a torus*, `arXiv:1303.3982`.

[31] A. Chatzistavrakidis, H. Steinacker and G. Zoupanos, *Intersecting branes and a standard model realization in matrix models*, *JHEP* **1109** (2011) 115 [`arXiv:1107.0265`].

[32] J. Nishimura and A. Tsuchiya, *Realizing chiral fermions in the type IIB matrix model at finite N*, `arXiv:1305.5547`.

[33] T. Hotta, J. Nishimura and A. Tsuchiya, *Dynamical aspects of large N reduced models*, *Nucl. Phys.* **B 545** (1999) 543 [`hep-th/9811220`].

[34] J. Ambjorn, K. N. Anagnostopoulos, W. Bietenholz, T. Hotta and J. Nishimura, *Large N dynamics of dimensionally reduced 4-D SU(N) super Yang-Mills theory*, *JHEP* **0007** (2000) 013 [`hep-th/0003208`].

[35] J. Ambjorn, K. N. Anagnostopoulos, W. Bietenholz, T. Hotta and J. Nishimura, *Monte Carlo studies of the IIB matrix model at large N*, *JHEP* **0007** (2000) 011 [`hep-th/0005147`].

[36] J. Ambjorn, K. N. Anagnostopoulos, W. Bietenholz, F. Hofheinz and J. Nishimura, *On the spontaneous breakdown of Lorentz symmetry in matrix models of superstrings*, *Phys. Rev.* **D 65** (2002) 086001 [`hep-th/0104260`].

[37] P. Bialas, Z. Burda, B. Petersson and J. Tabaczek, *Large N limit of the IKKT matrix model*, *Nucl. Phys.* **B 592** (2001) 391 [`hep-lat/0007013`].

[38] Z. Burda, B. Petersson and J. Tabaczek, *Geometry of reduced supersymmetric 4-D Yang-Mills integrals*, *Nucl. Phys.* **B 602** (2001) 399 [`hep-lat/0012001`].

[39] J. Ambjorn, K. N. Anagnostopoulos, J. Nishimura and J. J. M. Verbaarschot, *The factorization method for systems with a complex action: a test in random matrix theory for finite density QCD*, *JHEP* **0210** (2002) 062 [`hep-lat/0208025`].

[40] J. Ambjorn, K. N. Anagnostopoulos, J. Nishimura and J. J. M. Verbaarschot, *Noncommutativity of the zero chemical potential limit and the thermodynamic limit in finite density systems*, *Phys. Rev.* **D 70** (2004) 035010 [`hep-lat/0402031`].

[41] V. Azcoiti, G. Di Carlo, A. Galante and V. Laliena, *New proposal for numerical simulations of theta vacuum - like systems*, *Phys. Rev. Lett.* **89** (2002) 141601 [`hep-lat/0203017`].

[42] K. N. Anagnostopoulos, T. Azuma and J. Nishimura, *A general approach to the sign problem: the factorization method with multiple observables*, *Phys. Rev.* **D 83** (2011) 054504 [`arXiv:1009.4504`];
K. N. Anagnostopoulos, T. Azuma and J. Nishimura, *A study of the complex action problem in a simple model for dynamical compactification in superstring theory using the factorization method*, *PoS LATTICE* **2010** (2010) 167 [`arXiv:1010.0957`].

[43] K. N. Anagnostopoulos, T. Azuma and J. Nishimura, *A practical solution to the sign problem in a matrix model for dynamical compactification*, *JHEP* **1110** (2011) 126 [`arXiv:1108.1534`];
K. N. Anagnostopoulos, T. Azuma and J. Nishimura, *Towards an effective importance sampling in Monte Carlo simulations of a system with a complex action*, *PoS LATTICE* **2011** (2011) 181 [`arXiv:1110.6531`].

[44] Z. Fodor, S. D. Katz and C. Schmidt, *The density of states method at non-zero chemical potential*, *JHEP* **0703** (2007) 121 [`hep-lat/0701022`];
Z. Fodor and S. D. Katz, *A new method to study lattice QCD at finite temperature and chemical potential*, *Phys. Lett.* **B 534** (2002) 87 [`hep-lat/0104001`];
Z. Fodor and S. D. Katz, *Critical point of QCD at finite T and mu, lattice results for physical quark masses*, *JHEP* **0404** (2004) 050 [`hep-lat/0402006`].

[45] S. Ejiri, *On the existence of the critical point in finite density lattice QCD*, *Phys. Rev.* **D 77** (2008) 014508 [`arXiv:0706.3549`];
S. Ejiri, *Phase structure of hot dense QCD by a histogram method*, `arXiv:1306.0295`.

[46] M. P. Lombardo, K. Splittorff and J. J. M. Verbaarschot, *Distributions of the phase angle of the fermion determinant in QCD*, *Phys. Rev.* **D 80** (2009) 054509 [`arXiv:0904.2122`];
M. P. Lombardo, K. Splittorff and J. J. M. Verbaarschot, *The fluctuations of the quark number and of the chiral condensate*, *Phys. Rev.* **D 81** (2010) 045012 [`arXiv:0910.5482`].

[47] J. Greensite, J. C. Myers and K. Splittorff, *The QCD sign problem as a total derivative*, `arXiv:1306.3085`;
W. Unger, P. de Forcrand, *Continuous time Monte Carlo for lattice QCD in the strong coupling limit,"* *J. Phys.* **G 38** (2011) 124190 [`arXiv:1107.1553`];
P. de Forcrand, O. Philipsen, *Constraining the QCD phase diagram by tricritical lines at imaginary chemical potential*, *Phys. Rev. Lett.* **105** (2010) 152001 [`arXiv:1004.3144`];
J. Bloch, *A subset solution to the sign problem in random matrix simulations*, *Phys. Rev.* **D 86** (2012) 074505 [`arXiv:1205.5500`];
J. Bloch, *Evading the sign problem in random matrix simulations*, *Phys. Rev. Lett.* **107** (2011) 132002 [`arXiv:1103.3467`];
J. Bloch, T. Wettig, *The QCD sign problem and dynamical simulations of random matrices*, *JHEP* **05** (2011) 048 [`arXiv:1102.3715`];
G. Aarts, F. A. James, E. Seiler, I. -O. Stamatescu, *Complex Langevin: etiology and diagnostics of its main problem*, *Eur. Phys. J.* **C 71** (2011) 1756 [`arXiv:1101.3270`];
G. Aarts, F. A. James, *On the convergence of complex Langevin dynamics: the three-dimensional XY model at finite chemical potential*, *JHEP* **08** (2010) 020 [`arXiv:1005.3468`];
G. Aarts, *Can stochastic quantization evade the sign problem? The relativistic Bose gas at finite chemical potential*, *Phys. Rev. Lett.* **102** (2009) 131601 [`arXiv:0810.2089`];
G. Aarts and I. -O. Stamatescu, *Stochastic quantization at finite chemical potential*, *JHEP* **0809** (2008) 018 [`arXiv:0807.1597`];
S. Chandrasekharan, A. Li, *Fermion bag approach to the sign problem in strongly coupled lattice QED with Wilson fermions*, *JHEP* **01** (2011) 018 [`arXiv:1008.5146`];
C. R. Allton, S. Ejiri, S. J. Hands, O. Kaczmarek, F. Karsch, E. Laermann, C. Schmidt, L. Scorzato, *The QCD thermal phase transition in the presence of a small chemical potential*, *Phys. Rev.* **D 66** (2002) 074507 [`hep-lat/0204010`];
R. V. Gavai, S. Gupta, *Pressure and nonlinear susceptibilities in QCD at finite chemical potentials*, *Phys. Rev.* **D 68** (2003) 034506 [`hep-lat/0303013`];
M. D'Elia, M. -P. Lombardo, *Finite density QCD via imaginary chemical potential*, *Phys. Rev.* **D 67** (2003) 014505 [`hep-lat/0209146`];
P. de Forcrand, O. Philipsen, *The QCD phase diagram for small densities from imaginary chemical potential*, *Nucl. Phys.* **B 642** (2002) 290 [`hep-lat/0205016`];
W. Bietenholz, A. Pochinsky, U. J. Wiese, *Meron cluster simulation of the theta vacuum in the 2-d O(3) model*, *Phys. Rev. Lett.* **75** (1995) 4524 [`hep-lat/9505019`].

[48] M. Creutz, *Microcanonical Monte Carlo simulation*, *Phys. Rev. Lett.* **50** (1983) 1411;
G. Bhanot, K. Bitar and R. Salvador, *On solving four-dimensional SU(2) gauge theory by numerically finding its partition function*, *Phys. Lett.* **B 188** (1987) 246;
G. Bhanot, A. Gocksch and P. Rossi, *On simulating complex actions*, *Phys. Lett.* **B 199** (1987) 101;
A. Gocksch, *Simulating lattice QCD at finite density*, *Phys. Rev. Lett.* **61** (1988) 2054;
M. Karliner, S. R. Sharpe and Y. F. Chang, *Zeroing in on SU(3)*, *Nucl. Phys.* **B 302** (1988) 204;
A. Gocksch, *The Riemann walk: a method for simulating complex actions*, *Phys. Lett.* **B 206**

(1988) 290.

[49] J. Nishimura, *Exactly solvable matrix models for the dynamical generation of space-time in superstring theory*, *Phys. Rev.* **D 65**, 105012 (2002) [`hep-th/0108070`].

[50] J. Nishimura, T. Okubo and F. Sugino, *Gaussian expansion analysis of a matrix model with the spontaneous breakdown of rotational symmetry*, *Prog. Theor. Phys.* **114** (2005) 487 [`hep-th/0412194`].

[51] T. Aoyama, J. Nishimura and T. Okubo, *Spontaneous breaking of the rotational symmetry in dimensionally reduced super Yang-Mills models*, *Prog. Theor. Phys.* **125** (2011) 537 [`arXiv:1007.0883`].

[52] K. N. Anagnostopoulos, T. Azuma and J. Nishimura, *Monte Carlo simulations of a supersymmetric matrix model of dynamical compactification in non perturbative string theory*, *PoS LATTICE* **2012** (2012) 226 [`arXiv:1211.0950`].

[53] A. D. Kennedy, I. Horvath and S. Sint, *A new exact method for dynamical fermion computations with nonlocal actions*, *Nucl. Phys. Proc. Suppl.* **73** (1999) 834 [`hep-lat/9809092`];
M. A. Clark and A. D. Kennedy, *The RHMC algorithm for two flavors of dynamical staggered fermions*, *Nucl. Phys. Proc. Suppl.* **129** (2004) 850 [`hep-lat/0309084`];
M. A. Clark, A. D. Kennedy and Z. Sroczynski, *Exact 2+1 flavour RHMC simulations*, *Nucl. Phys. Proc. Suppl.* **140** (2005) 835 [`hep-lat/0409133`].

[54] M. A. Clark and A. D. Kennedy, `https://github.com/mikeaclark/AlgRemez`, 2005.

[55] S. Catterall and S. Karamov, *Testing a Fourier accelerated hybrid Monte Carlo algorithm*, *Phys. Lett.* **B 528** (2002) 301 [`hep-lat/0112025`].

[56] B. Jegerlehner, *Krylov space solvers for shifted linear systems*, `hep-lat/9612014`.